

Review

In-Situ Polymerized Solid-State Polymer Electrolytes for High-Safety Sodium Metal Batteries: Progress and Perspectives

Sijia Hu ^{1,2,3,4,†}, Duo Wang ^{1,2,3,4,†}, Zhixiang Yuan ^{1,3,4,5,†}, Hao Zhang ^{1,3,4}, Songwei Tian ^{1,3,4}, Yalan Zhang ^{1,3,4}, Botao Zhang ⁵, Yongqin Han ², Jianjun Zhang ^{1,3,4,*} and Guanglei Cui ^{1,3,4,*} 

¹ Qingdao Industrial Energy Storage Research Institute, Qingdao Institute of Bioenergy and Bioprocess Technology, Chinese Academy of Sciences, Qingdao 266101, China

² School of Materials Science and Engineering, Shandong University of Science and Technology, Qingdao 266590, China

³ Shandong Energy Institute, Qingdao 266101, China

⁴ Qingdao New Energy Shandong Laboratory, Qingdao 266101, China

⁵ School of Chemistry and Chemical Engineering, Qingdao University, Qingdao 266071, China

* Correspondence: zhang_jj@qibebt.ac.cn (J.Z.); cuigl@qibebt.ac.cn (G.C.)

† These authors contributed equally to this work.

Abstract: The practical usage of sodium metal batteries is mainly hampered by their potential safety risks caused by conventional liquid-state electrolytes. Hence, solid-state sodium metal batteries, which employ inorganic solid electrolytes and/or solid-state polymer electrolytes, are considered an emerging technology for addressing the safety hazards. Unfortunately, these traditional inorganic/polymer solid electrolytes, most of which are prepared via ex-situ methods, frequently suffer from inadequate ionic conductivity and sluggish interfacial transportation. In light of this, in-situ polymerized solid-state polymer electrolytes are proposed to simplify their preparation process and simultaneously address these aforementioned challenges. In this review, the up-to-date research progress of the design, synthesis, and applications of this kind of polymer electrolytes for sodium batteries of high safety via several in-situ polymerization methods (including photoinduced in-situ polymerization, thermally induced in-situ free radical polymerization, in-situ cationic polymerization, and cross-linking reaction) are summarized. In addition, some perspectives, opportunities, challenges, and potential research directions regarding the further development of in-situ fabricated solid-state polymer electrolytes are also provided. We expect that this review will shed some light on designing high-performance solid-state polymer electrolytes for building next-generation sodium batteries with high safety and high energy.

Keywords: solid-state polymer electrolyte; in-situ polymerization; sodium metal batteries; high safety; stable interfacial chemistry



Citation: Hu, S.; Wang, D.; Yuan, Z.; Zhang, H.; Tian, S.; Zhang, Y.; Zhang, B.; Han, Y.; Zhang, J.; Cui, G. In-Situ Polymerized Solid-State Polymer Electrolytes for High-Safety Sodium Metal Batteries: Progress and Perspectives. *Batteries* **2023**, *9*, 532. <https://doi.org/10.3390/batteries9110532>

Academic Editors: Stefan Adams and Seung-Wan Song

Received: 20 July 2023

Revised: 8 September 2023

Accepted: 20 October 2023

Published: 26 October 2023



Copyright: © 2023 by the authors. Licensee MDPI, Basel, Switzerland. This article is an open access article distributed under the terms and conditions of the Creative Commons Attribution (CC BY) license (<https://creativecommons.org/licenses/by/4.0/>).

1. Introduction

Sodium-ion batteries (SIBs) are one of the auspicious alternatives to state-of-the-art lithium-ion batteries (LIBs) because of the natural plenitude of sodium (Na) in the Earth's crust. Additionally, SIBs can be discharged to 0 V without causing overdischarge issues, which greatly improves their safety properties for their deployment for electric vehicles. Moreover, SIBs could employ cheaper aluminum as current collectors instead of copper, which greatly reduces the cost of SIBs. In the last, SIBs usually possess a longer service life, higher rate performance, and wider operating temperature range compared with LIBs [1–3]. With the rapid growth of plug-in or hybrid electric vehicles and large-format green energy storage power stations, high-energy and high-safety SIBs are urgently desired [4–6]. To remarkably improve the energy density of SIBs, significant research efforts have been dedicated to finding and identifying suitable electrode materials and several promising types of cathodes (e.g., layered transition metal oxides, sodium fluorophosphates,

etc.) and anode materials (carbonaceous materials, sodium alloys, and transition metal oxides/sulfides) have been identified [7–10]. In contrast, less attention has been paid to developing reliable electrolytes, which are also important in guaranteeing improved battery performance and safety property of SIBs [11–13]. It is also worth noting that the conventional liquid-state electrolytes (such as carbonate electrolytes, ether electrolytes, etc.) are plagued by their severe safety risks because of the potential electrolyte leakage and even combustion [14,15]. Consequently, developing new kinds of highly safe electrolytes is highly desirable for building high-energy and high-safety SIBs [16,17].

Solid-state electrolytes are believed to effectively relieve the unsafe factors brought by conventional liquid-state electrolytes. Solid-state electrolytes include inorganic solid-state electrolytes and solid-state polymer electrolytes. Even though the inorganic solid-state electrolytes possess ionic conductivity that is comparable to or even higher than that of liquid-state electrolytes at room temperature, its practical application is limited due to the high brittleness and poor interfacial contact. In contrast, solid-state polymer electrolytes exhibit better electrode–electrolyte interfacial compatibility, flexibility, and processability. From the material’s point of view, the solid-state polymer electrolytes (SPEs), which also possess superior thermal stability characteristics, are expected to be the ideal electrodes for building high-safety solid-state SIBs. In addition, their wide electrochemical window is also advantageous to enable a compatible and stable electrode–electrolyte interface [18,19]. Hence, the SPEs are recognized as one of the promising candidates to replace the traditional liquid-state electrolytes for SIBs.

Until now, a series of polymer matrices including poly(ethylene oxide) [20], poly(vinylidene fluoridehexafluoro propylene) [21], poly(acrylonitrile) [22], poly(methyl vinyl ether-alt-maleic anhydride) [23], and other new polymers [24–36] have been proposed and prepared as SPEs for LIBs and SIBs. Nevertheless, these above-stated SPEs are prepared mainly by ex-situ preparation methods (e.g., solution-casting method), which are time-consuming and complicated. Furthermore, these ex-situ-prepared SPEs frequently suffer from high interfacial resistance [37]. Compared with the ex-situ preparation methods for manufacturing SPEs, the in-situ polymerization technique, which converts the injected liquid precursor into a solid electrolyte in situ through chemical or electrochemical reactions during the cell manufacturing procedures, is widely acknowledged to address the high interfacial resistance challenge [38,39]. Hence, this technique has drawn much attention recently for preparing various SPEs [40–48]. During a typical in-situ polymerization process, liquid precursors are firstly injected into the batteries, and then they are progressively converted into SPEs initiated under the photo-, chemical, or cationic initiators conditions [49]. Because of this, compared with these ex-situ prepared SPEs, the as-obtained SPEs can sufficiently infiltrate into the electrodes and conformal and excellent solid–solid contact between the SPEs and the electrodes is accordingly guaranteed. Moreover, considering that the polymerized electrolyte does not suffer from electrolyte leakage compared with the liquid-state electrolyte, improved safety performance is achieved [50,51]. Some review papers focusing on ex-situ polymerized SPEs for SIBs have been previously reported [52–55], with insufficient attention paid to the in-situ polymerization techniques. Therefore, summarizing and prospecting the in-situ polymerization methods for preparing the SPEs is necessary. In this retrospect, a comprehensive review of the research progress in the design, synthesis, and applications of SPEs for high-safety sodium metal batteries (SMBs) via in-situ polymerization (including photoinduced polymerization [56–64], thermally induced free radical polymerization [65–76], cationic polymerization [77–79], and cross-linking reaction [80]) is presented in this review (Table 1), aiming to further boost the rapid development of the SPEs for SMBs. Meanwhile, the application challenges and potential opportunities of the in-situ polymerization techniques are also provided. The review ends with an in-depth discussion on the remaining challenges and possible solutions for the in-situ polymerization methods for building high-safety SMBs. It is expected that this review will guide the designing of in-situ polymerized high-performance SPEs for building high-safety and high-energy SMBs.

Table 1. Ionic conductivities of the in-situ polymerized solid-state polymer electrolytes.

Initiation Conditions	Solid-State Polymer Electrolyte	Ionic Conductivity σ , S/cm	Transference Number	Test Temperature	Ref
photoinduced	BEMA/PEGMA	5.1×10^{-3}	0.53	20 °C	[56]
	PEGDMA-NaFSI-SPE	1.1×10^{-4}		30 °C	[57]
	ETPTA-based SPE	1.2×10^{-3}	0.62	room temperature	[58]
	(PETEA-THEICTA)-based SPE	3.85×10^{-3}	0.34	25 °C	[59]
thermally induced	PVC-CPE	1.2×10^{-4}	0.6	25 °C	[62]
	PMMA-based GPE	6.2×10^{-3}		25 °C	[63]
	TMPTA-based SPE	7.16×10^{-4}	0.62	30 °C	[64]
	poly(BA)-based SPE	1.6×10^{-3}	0.39	room temperature	[65]
	HPISE	1.15×10^{-3}		25 °C	[66]
	(PEGMA)-based SPE	9.1×10^{-4}	0.24	27 °C	[67]
	(PCL-TA)-based SPE	6.3×10^{-3}		room temperature	[68]
cationic induced	(MADEMP)-based SPE	3.37×10^{-3}	0.52	room temperature	[72]
	PPDE-CPE	1.2×10^{-3}	0.46	room temperature	[77]
	GPE-CPN	8.2×10^{-4}	0.46	room temperature	[78]
	DOL-based SPE	3.66×10^{-4}	0.66	room temperature	[79]

The abbreviations in the table are explained below: BEMA: bisphenol A ethoxylate dimethacrylate; PEGMA: poly(ethylene glycol) methyl ether methacrylate; PEGDMA: poly(ethylene glycol) methyl ether methacrylate; ETPTA: ethoxylated trimethylolpropane triacrylate; PETEA: poly(S-pentaerythritol tetraacrylate); THEICTA: tris [2-(acryloyloxy)ethyl] isocyanurate; PVC-CPE: poly(vinylene carbonate)-based composite polymer electrolyte; TMPTA: trihydroxymethylpropyl triacrylate; poly(BA): poly(butyl acrylate)-based GPE; HPISE: hierarchical poly (ionic liquid)-based solid electrolyte; PEGMA: Poly(ethylene glycol) methyl ether methacrylate; PCL-TA: polycaprolactone triacrylate; MADEMP: multifunctional di(2-methylacryloyldioxyethyl)methyl phosphonate; PPDE-CPE: polysulfonamide-supported poly(ethylene glycol) divinyl ether-based polymer electrolyte; GPE-CPN: gel polymer electrolyte with a cross-linked polyether network; DOL: 1,3-Dioxolane.

2. SPEs Prepared Using Photoinduced In-Situ Polymerization

The earliest research on SMBs using photoinduced in-situ polymerized SPEs dates back to 2015. Federico et al. demonstrated a gel polymer electrolyte using di-methacrylate oligomer (i.e., bisphenol A ethoxylate dimethacrylate, BEMA) and poly (ethylene glycol) methyl ether methacrylate (PEGMA) polymer matrices and Irgacure 1173 photo-initiator (2 wt.%) [56]. It was confirmed using the Fourier transform infrared (FTIR) that the photoinduced polymerization reaction was accomplished in no more than 5 min with 100% conversion. The results imply that this in-situ polymerization process is much faster compared with the conventional preparation processes for fabricating polymer membranes (such as solvent casting and melt flow).

The prepared BEMA/PEGMA-based photopolymer electrolyte was characterized by the authors, and they found that it exhibited high ionic conductivity (5.1 mS cm^{-1} at 20 °C), excellent sodium ion transportability (sodium-ion transference number, 0.53 ± 0.05 , 20 °C), stable interfacial characteristics, and a wider electrochemical stability window (4.8 V versus Na/Na⁺). Considering that thermal stability is also one of the key factors affecting its successful application in SMBs, the authors also conducted thermogravimetric analysis (TGA), and the results implied that the prepared BEMA/PEGMA-based photopolymer electrolyte possessed good thermal stability for SMBs. The authors assembled TiO₂-based cells using the BEMA/PEGMA-based photopolymer electrolyte and conducted electrochemical cycling tests. The cycling test displayed that the studied cell delivered stable capacity exceeding 50 mAh g⁻¹ after 250 cycles at 1 mA cm⁻², proving the decent electrochemical cycling performance of the as-prepared BEMA/PEGMA-based photopolymer electrolyte.

In 2020, Yu et al. reported fabricating solid-state SMBs using flexible SPE, which was in-situ polymerized using poly(ethylene glycol) methyl ether methacrylate (PEGDMA) monomer and sodium bis(fluorosulfonyl)imide (NaFSI) sodium salt as well as the 2,2-dimethoxy-2-phenylacetophenone (DMPA, 1 wt%) photoinitiator (as-obtained PEGDMA-NaFSI-SPE) [57]. This report showcased the probability of building flexible wearable

solid-state SMBs using the in-situ polymerization methods. The ionic conductivity of the designed PEGDMA-NaFSI-SPE was $1.1 \times 10^{-4} \text{ S cm}^{-1}$ at 30°C . The as-obtained PEGDMA-NaFSI-SPE exhibited both high ionic conductivity and good electrolyte–electrode interface bonding. Moreover, the authors used density functional theory (DFT) calculations to study the Na^+ migration barrier in $\text{Na}_3\text{V}_2(\text{PO}_4)_3$ (NVP) (Figure 1a,c) and PEGDMA-NaFSI-SPE (Figure 1b,d), as shown in Figure 1. This figure suggests that the Na^+ transportation barrier in PEGDMA-NaFSI-SPE is much lower than that in the NVP cathode, which indicates a high-rate capability can be obtained using the prepared electrolyte. Benefiting from these merits, the built battery delivered a specific capacity of 106 mAh g^{-1} at 0.5 C even after repeated bending for 535 cycles.

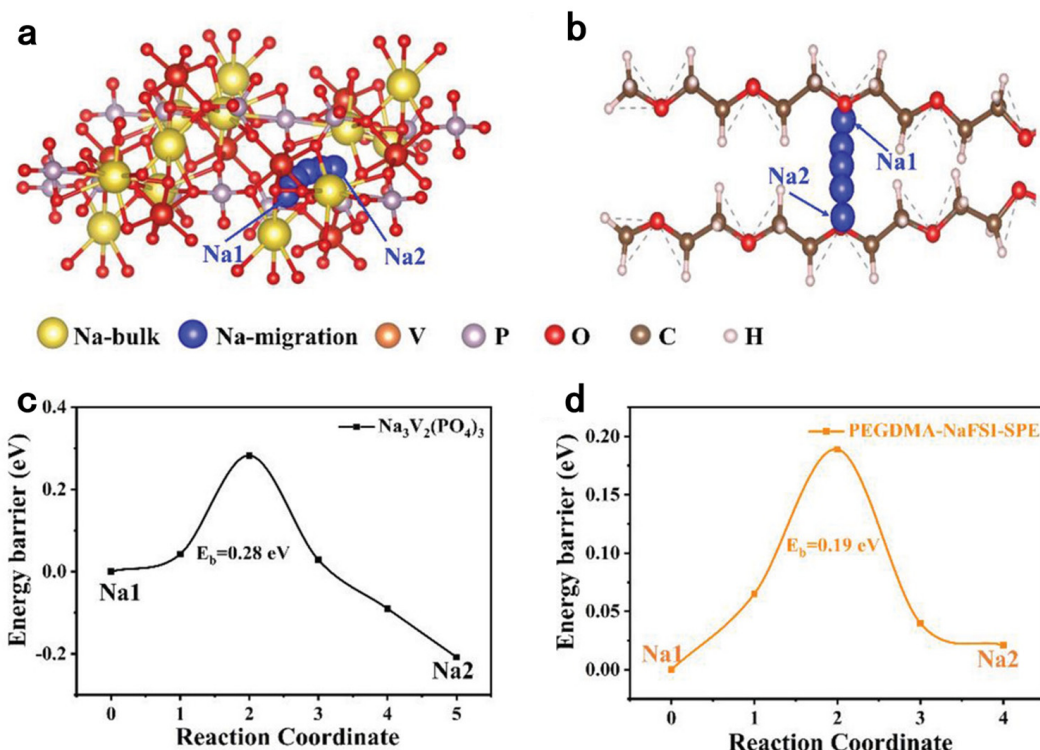


Figure 1. Schematic structure explaining the optimized Na^+ transportation in (a) NVP and (b) PEGDMA-NaFSI-SPE. The calculated migration energy for Na^+ moving from Na1 to Na2 site in (c) NVP and (d) PEGDMA-NaFSI-SPE. Reproduced with permission from [57].

To further improve the Na^+ ionic conductivity and extend the electrochemical window of the traditional SPEs, Wen et al. reported a new kind of ethoxylated trimethylolpropane triacrylate (ETPTA)-based SPE [58]. The preparation process and the corresponding characterization results are vividly illustrated in Figure 2a–d. One can note that the UV light successfully triggered ETPTA polymerization to form SPE, which was confirmed by the FTIR result showing the disappearance of the C=C bond of ETPTA after UV curing. The obtained SPE exhibited a high electrochemical oxidation voltage (>4.7 V versus Na^+/Na), and its ionic conductivity at room temperature reached 1.2 mS cm^{-1} . Owing to its high ionic conduction and the improved interfacial NVP/Na compatibility, the built batteries employing such SPE could maintain high specific capacity of 55 mAh g^{-1} at 15 C and provide a high discharge specific capacity of 98 mAh g^{-1} even after 1000 cycles (capacity retention of 96%). No electrolyte leakage and/or internal short circuit was detected using this ETPTA-based SPE in both folding and reflatting state, demonstrating its excellent flexibility and exceptional safety.

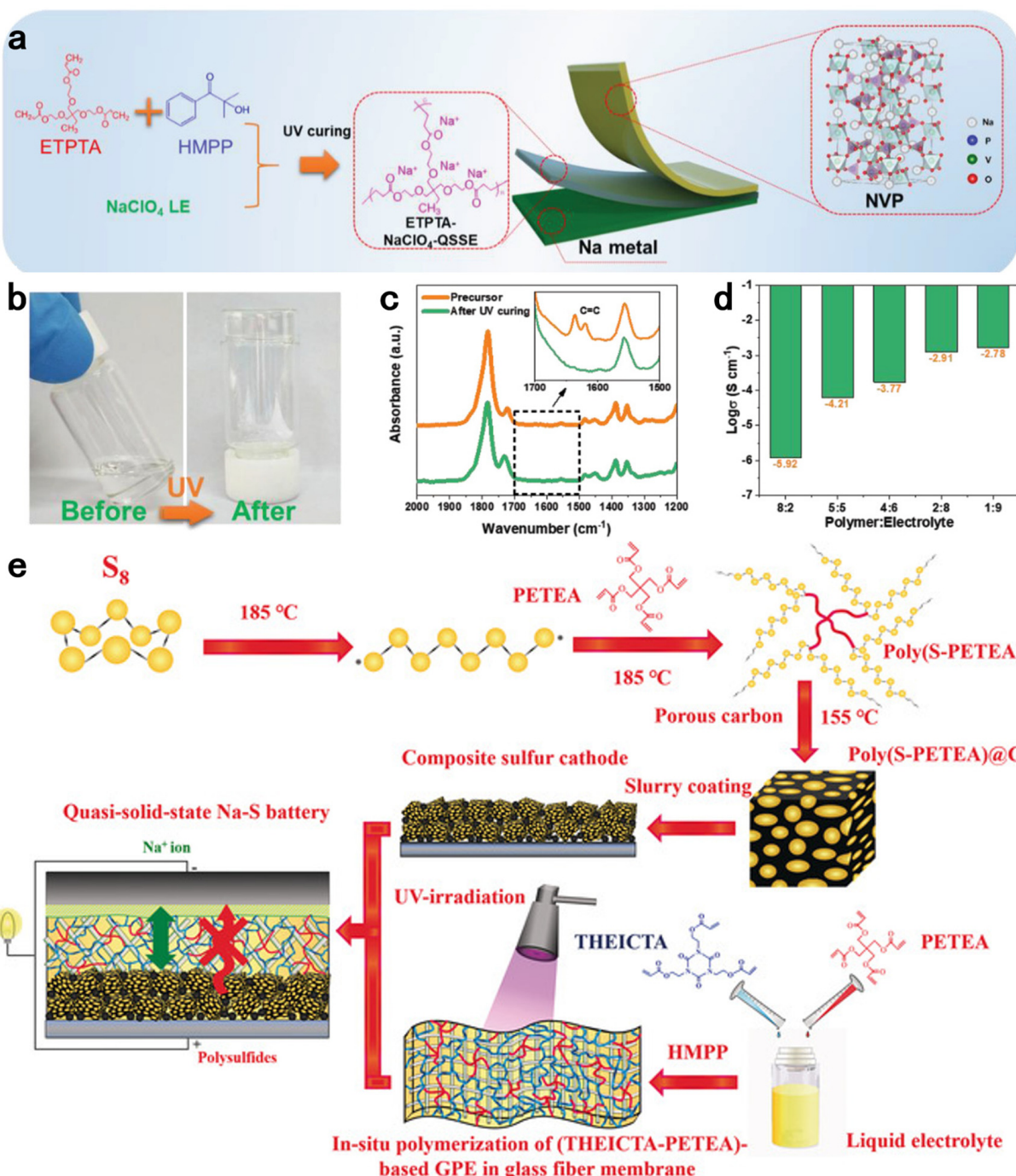


Figure 2. (a) Schematic explaining the ETPTA-based SPE and NVP|ETPTA-based SPE|Na SMBs. Characterization results of the ETPTA-based SPE using (b) Optical microscopy and (c) FTIR before and after UV curing. (d) The measured ionic conductivity of the ETPTA-based SPE consisting of varying degrees of polymer/electrolyte components. Reproduced with permission from [58]. (e) Schematic explaining the assembly process of the Na-S battery. Reproduced with permission from [59].

This work suggests that utilizing the in-situ polymerization strategy to manufacture SPEs is a new direction for developing high energy-density, flexible, and room-temperature solid-state SMBs. Nevertheless, it should be mentioned that the NVP loading is only 1 mg cm^{-2} , which may not be sufficient for practical usage. Hence, in the future, high mass-loading ($\geq 20 \text{ mg cm}^{-2}$) of cathodes is suggested to be used in building and testing SMBs.

Zhou et al. used 2-hydroxy-2-methyl-1-phenyl-1-propanone (HMPP) as the photo-initiator to manufacture the (pentaerythritol tetraacrylate-tris[2-(acryloyloxy)ethyl]isocyanurate) (PETEA-THEICTA)-based SPE via in-situ photoinitiated polymerization [59]. Compared with the conventional liquid-state electrolytes, the as-prepared SPE displayed higher electrochemical stabilities. It also showed high thermal stability, ionic conductivity (3.85 mS cm^{-1} at 25°C), and sodium-ion transference number (0.34). These results suggest that the as-prepared SPE may enable a stable Na electrodeposition and reduce the polarization of polymer cells. These merits may also meet the requirement for building solid-state sodium-sulfur batteries. To confirm this, the authors built several solid-state cells and tested their performance. The test results showed that the built Na symmetrical cell could run stably up to 300 h during the battery cycling at 0.1 mA cm^{-2} . They also prepared the S rich poly(S-PETEA) composite sulfur cathode (poly(S-PETEA)@C) via copolymerizing S₈ with PETEA, as shown in Figure 2e. And, the authors assembled Na/SPE/poly(S-PETEA)@C cell and tested its performance. It was shown that this cell possesses a high coulombic efficiency (almost 100%) and maintains nearly 750 mAh^{-1} after one hundred cycles.

These abovementioned works imply that the photoinduced in-situ polymerization is advantageous to construct advanced SPEs. However, in light of the fact that ultraviolet light cannot penetrate the battery shell, it is still a difficulty to directly build solid-state SMBs using photoinduced in-situ polymerization. In the future, other types of rays (e.g., gamma rays) with stronger penetration capability and more suitable precursors can be selected to realize the in-situ polymerization of SMBs.

3. SPEs Prepared by Thermally Induced In-Situ Free Radical Polymerization

In this section, we will concentrate mainly on the research progress of the SPEs manufactured by thermally induced in-situ free radical polymerization, which is a widely used strategy for preparing SPEs. Several categories of such polymer electrolytes will be included: conventional polymer electrolytes, poly(ionic liquid)-based polymer electrolytes, and flame-retardant polymer electrolytes.

3.1. Conventional Polymer Electrolytes

Most of the vinyl monomers can be polymerized into high-mass polymers using the thermally induced in-situ free radical polymerization process. For example, vinylene carbonate (VC), an effective additive of lithium/sodium batteries, can be polymerized to high-molecular-mass polymer via free radical polymerization.

In light of this, Chen et al. prepared a poly(vinylene carbonate)-based composite polymer electrolyte (PVC-CPE) for ambient temperature solid-state batteries for the first time [62]. This PVC-CPE exhibited high ionic conductivity at 25°C (0.12 mS cm^{-1}), high Na^+ transference number (0.60), and decent interfacial stability between the electrode and the electrolyte. It was reported that the solid-state $\text{NaNi}_{1/3}\text{Fe}_{1/3}\text{Mn}_{1/3}\text{O}_2/\text{PVC-CPE/Na}$ battery, which was built using a facile in-situ polymerization method, presented a discharge capacity retention of 86.8% after 250 cycles at 0.2 C and 71.8% after 200 cycles at 1 C, suggesting that the as-prepared PVC-CPE is favorable for building ambient temperature solid-state SMBs.

Goodenough et al. synthesized a cut-price gel-polymer electrolyte of cross-linked PMMA by in situ polymerization and tested in a sodium-ion full-cell $\text{Sb}/\text{Na}_3\text{V}_2(\text{PO}_4)_3$ [63]. On account of promoting the gelation of organic solvents and helping the solvation of electrolytic ions, the PMMA chains are actually crucial components of the gel-polymer electrolyte. Moreover, the sodium ion full-cell delivered a capacity of 106.8 mAh g^{-1} at 0.1 C and also showed a capacity of 86.3 mAh g^{-1} with the coulombic efficiency approaching 100% after 100 charge-discharge cycles. Furthermore, when tested at an elevated temperature of 60°C , the cycling performance of the sodium-ion full-cell $\text{Sb}/\text{Na}_3\text{V}_2(\text{PO}_4)_3$ could be improved obviously by the presence of the gel-polymer electrolyte instead of liquid electrolyte.

Zhou et al. built high cathode mass loading SMBs by using trihydroxymethylpropyl triacrylate (TMPTA)-based electrolytes [64]. Intimate and conformal solid–solid contact between the electrodes and the SPE, which is conducive to the Na^+ migration, was achieved via the in-situ polymerization. Figure 3a–c shows that the as-prepared SPE could be paired with high-voltage cathode materials via in-situ interlocking the interfaces. Since the cathode mass loading is high, this strategy is favorable to developing high energy density SMBs with high mass loading. The built solid-state SMBs using this SPE remained at 80% capacity retention after 1000 cycles at 1 C at 60 °C. The built batteries also maintained 98% capacity retention after 100 cycles at 1 C, even at 0 °C, showing excellent temperature suitability of this in-situ formed SPE.

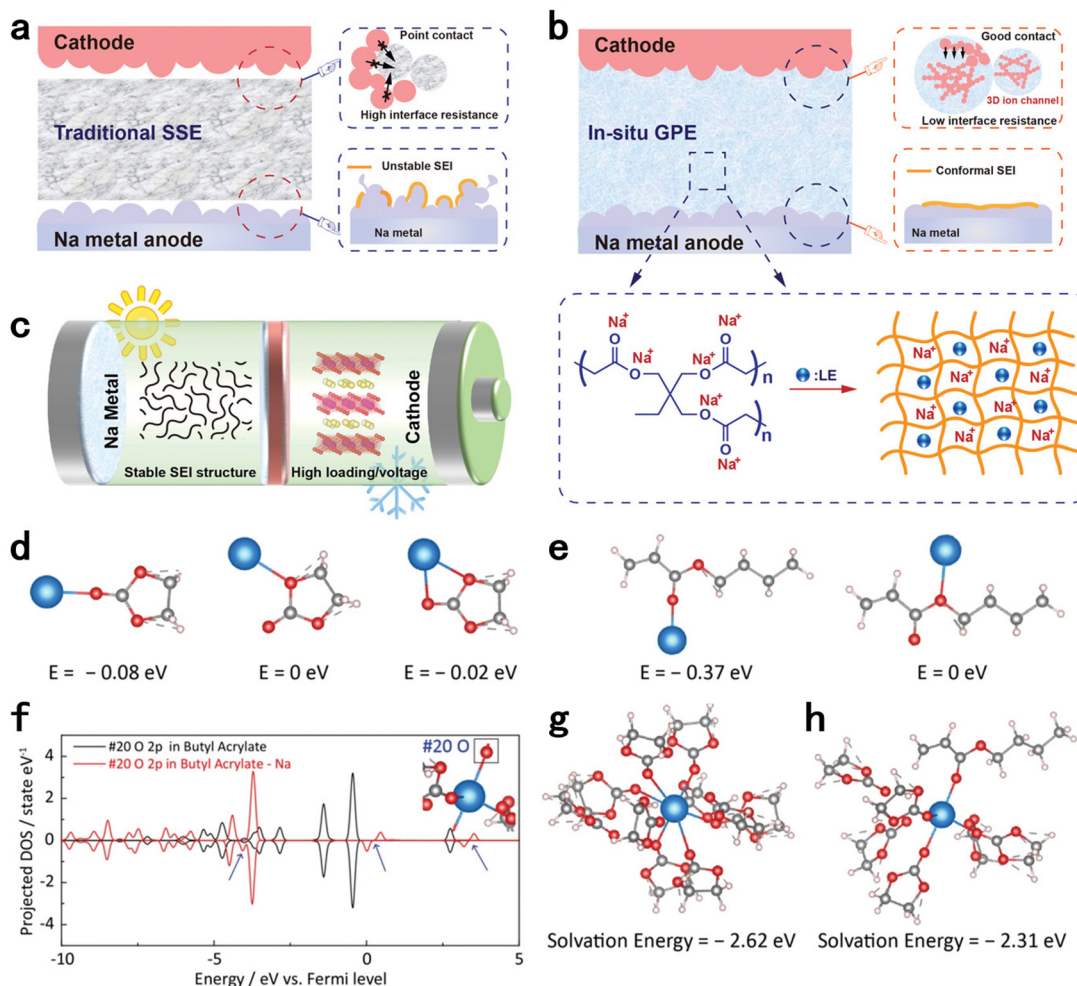


Figure 3. Illustration explaining the interlocked interface of the in-situ polymerized SPE, with the conventional solid–state interface as a comparison. (a) Schematic illustrating the unstable and poor interface. (b) Schematic illustrating the interlocked interface. (c) Schematic of the built battery. Reproduced with permission from [64]. The coordinates of (d) Na–EC and (e) Na–BA. (f) Total density of states (DOS) of BA and Na-BA and the optimized Na solvation structure in (g) LE and (h) SPE. The blue, red, gray, and white balls denote the Na, O, C, and H atoms. Reproduced with permission from [65].

Similarly, Zhang et al. reported a poly(butyl acrylate)-based SPE [65]. DFT calculations were used to study the coordination environment of Na^+ in this SPE, and the results are shown in Figure 3d–h, with the liquid electrolyte (LE) as the control sample. The optimized solvation structures of Na in LE and SPE are displayed in Figure 3g,h. This comparison showed that the solvation energy of Na is reduced in this SPE, indicating an improved

reaction kinetics in this SPE. As a result, the built NVP | SPE | Na battery displayed improved performance compared with that using LE.

It has to be noted that these three abovementioned polymer electrolytes are flammable, which is unfavorable to the safety of SMBs. Hence, it is suggested that more efforts are needed to develop promising flame-retardant polymer electrolytes for safe SMBs.

3.2. Poly(ionic liquid)-Based Polymer Electrolytes

Besides these common organic polymers mentioned above, poly(ionic liquid)s can also be utilized to manufacture SPEs. Ionic liquids are suitable candidates for in-situ preparing high-performance SPEs due to their merits of low volatility, nonflammability, sufficient electrochemical stability window, and relatively high ionic conductivity.

In this regard, Zhou et al. reported a hierarchical poly (ionic liquid)-based SPE for SMBs [66]. This SPE was manufactured via in-situ polymerizing 1,4-bis[3-(2-acryloyloxyethyl)imidazolium-1-yl]butane bis[-bis(trifluoromethanesulfonyl)imide] (C1-4TFSI) monomer in the 1-ethyl-3-methylimidazolium bis(trifluoromethanesulfonyl)imide (EMITFSI)-based electrolyte (HPILSE). And the as-prepared polymer electrolyte was later filled in the poly(diallyldimethylammonium) bis(trifluoromethanesulfonyl)imide (PDDATFSI) porous membrane (Figure 4). The elaborately designed SPE delivered high ionic conductivity (1.15 mS cm^{-1} at 25°C), satisfied oxidation window (4.6 V vs. Na/Na^+), sufficient mechanical strength, and intrinsic flame retardancy. Additionally, the full cells built with this SPE exhibited high-capacity retention of 85.5% after 100 cycles and high average coulombic efficiency at 0.1 C.

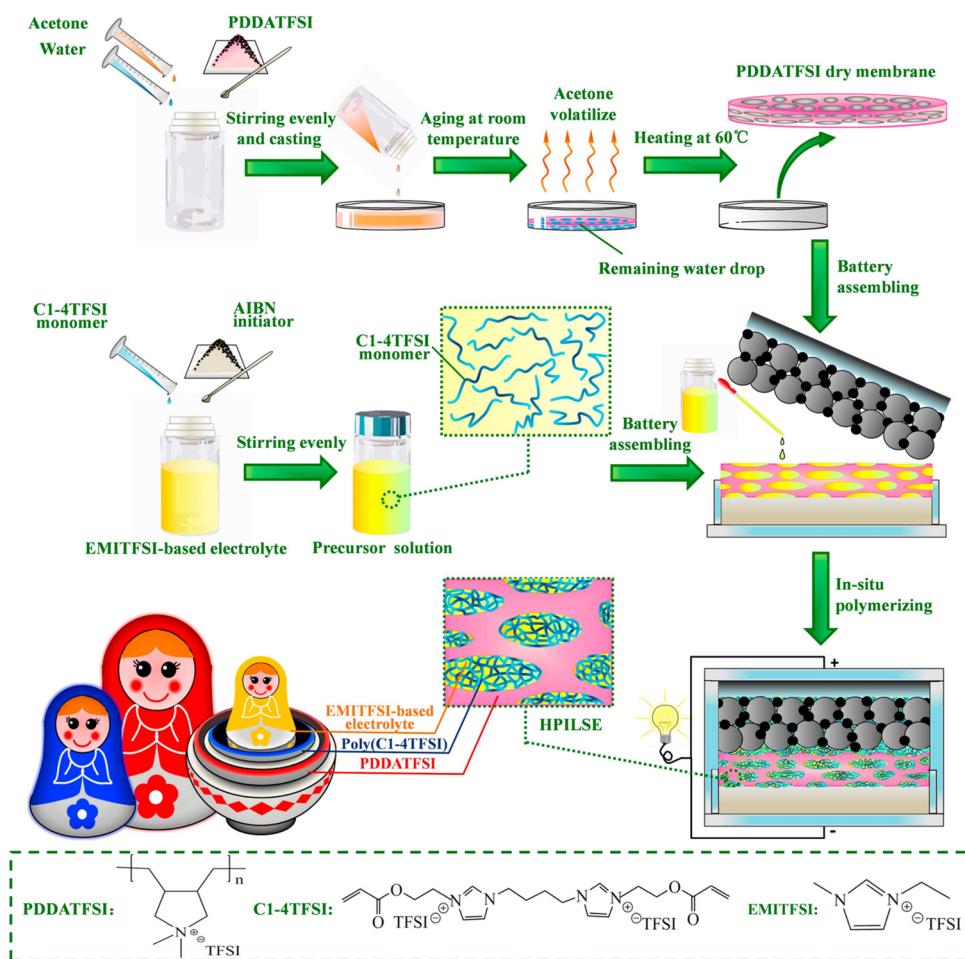


Figure 4. Schematic explaining the HPILSE. Reproduced with permission from [66].

Each type of SPE matrix features its own advantages and disadvantages. The high cost and cumbersome preparation process of ionic liquids-based polymer electrolytes have greatly limited their further development. In this regard, advanced eutectogel polymer electrolytes of low-cost and flame-retardant properties may be a future development direction.

3.3. Flame-Retardant Polymer Electrolytes

In recent years, in-situ formed flame-retardant polymer electrolytes have attracted much interest in SMBs. These flame-retardant SPEs can be mainly categorized into two types: (1) Triethyl phosphate (TEP) or trimethyl phosphate (TMP)-based SPE [67,68] and (2) Flame retardant polymer electrolytes formed by polymerization of unsaturated phosphate monomers [69–72].

For the former type, Chen et al. demonstrated a flexible poly(ethylene glycol) methyl ether methacrylate (PEGMA)-based SPE [67]. Figure 5a,b depicts the in-situ thermally induced polymerization process. The optimized flame-retardant electrolyte, PGT32-5% (ratio of PEGMA, TEP, and fluoroethylene carbonate (FEC) is 3:2:5%), exhibited high ionic conductivity and extended electrochemical window and excellent mechanical strength. In addition, the built full battery delivered a high-capacity retention. The introduction of FEC is beneficial to improve the electrode–electrolyte interface compatibility. In a similar way, Park et al. [68] also reported a nonflammable SPE prepared via in-situ cross-linking polycaprolactone triacrylate (PCL-TA) and TMP (Figure 5c).

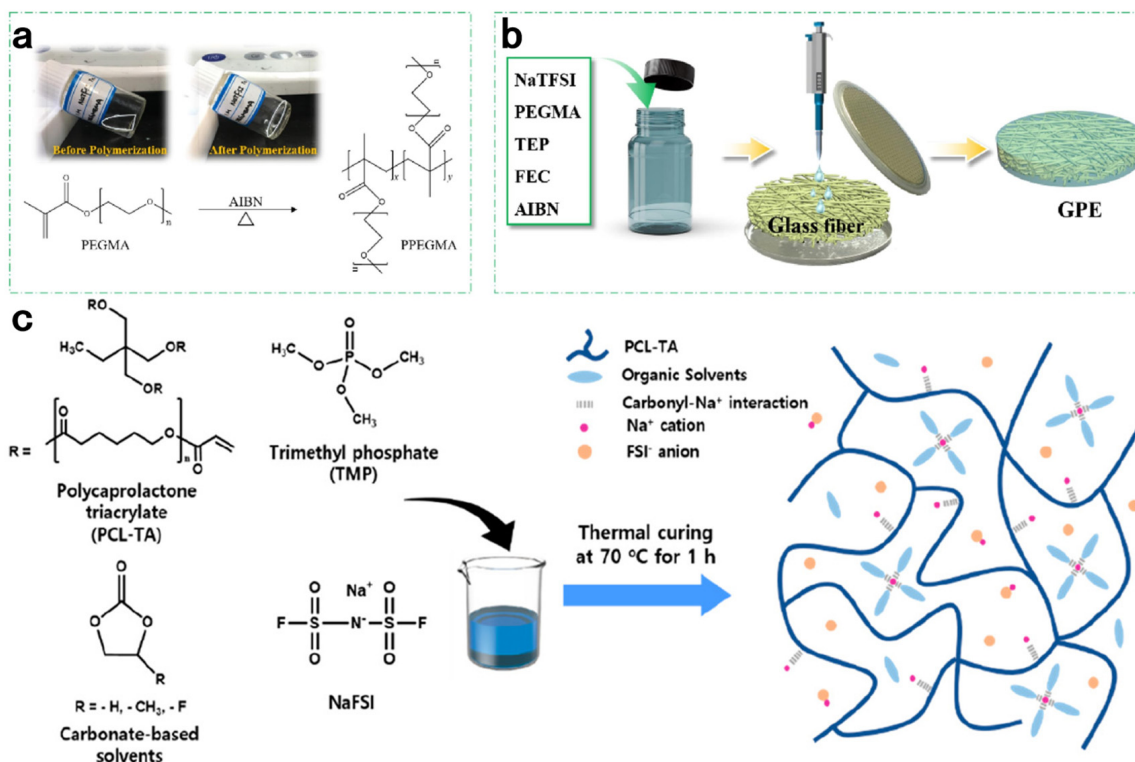


Figure 5. Schematic explaining (a) synthesizing PPEGMA and (b) GPEs. Reproduced with permission from [67]. (c) Schematic explaining synthesizing nonflammable GPE. Reproduced with permission from [68].

These two flame-retardant SPEs are compromised by the existence of small combustible molecules. Hence, Zheng et al. carried out a variety of systematic studies to design and fabricate the intrinsically flame-retardant SPEs [69–72]. In 2021, Zheng et al. reported stable di(2-methylacryloyldioxyethyl) methyl phosphonate (MADEMP)-based gel terpolymer electrolytes (Figure 6a) [72]. The electrostatic potential (ESP, which is closely related to the charge distribution of a molecule) distribution results of the polymer structural units are

displayed in Figure 6b–d, which contain the scenarios before and after Na^+ were bonded. The ESP result shows that it is mainly the MADEMP unit that coordinates with Na^+ , and the sodium ions transportation occurs through the coordinated sites of MADEMP and Na^+ in the polymer chain. Such polymer structural units are favorable to achieving high sodium ion conductivity. Furthermore, the structure may also prevent sodium dendrite growth. For these reasons, the built NVP/Na full cell exhibited high-capacity retention of 85.5% after 3500 cycles.

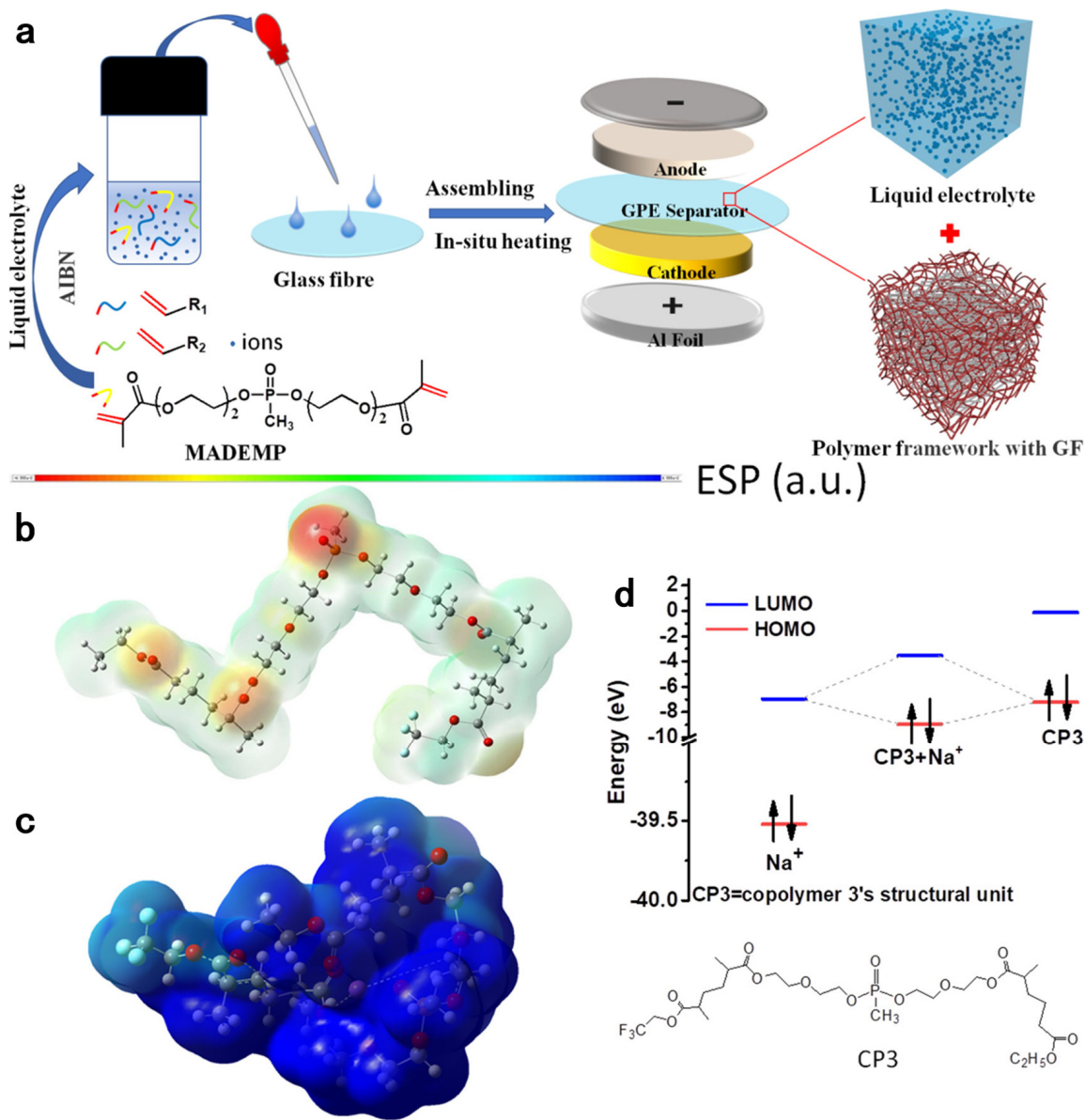


Figure 6. (a) Schematic explaining synthesizing SPEs. ESP results of the polymer 3: (b) before and (c) after binding the sodium ion, and (d) the highest occupied molecular orbital–lowest unoccupied molecular orbital (HOMO–LUMO) energy. O: red; C: gray; H: white; P: yellow; F: light blue; Na: purple. Reproduced with permission from [72].

As stated above, the multifunctional phosphonate-containing polymer electrolytes provide a lot of opportunities for preparing flame-retardant SPEs for SMBs. However, the incompatibility between the phosphate ester and the sodium metal limits its further practical application, which will be the focus of future work.

4. SPEs Manufactured Using In-Situ Cationic Polymerization

The research progress of SPEs prepared via photoinduced in-situ polymerization and thermally induced in-situ free radical polymerization for SMBs is reviewed in the previous parts. As stated above, the thermally induced in-situ free radical polymerization is widely used for preparing in-situ formed polymer electrolytes for SMBs. However, this strategy usually requires additional initiators (e.g., AIBN) and high-temperature conditions (e.g., 80 °C), both of which are unfavorable to achieving large-scale production under mild conditions. In contrast, in-situ cationic polymerization employs sodium salts as an initiator, bypassing the potential heating and/or ultraviolet irradiation damage during the in-situ polymerization. So far, there are a few in-situ cationic polymerized SPE for SMBs. In this part, the research advance of the in-situ cationic polymerized SPE for SMBs from the perspective of poly(ethylene glycol) divinyl ether and 1,3-dioxolane (DOL), together with their corresponding performance improvement principles are summarized.

In 2017, Zhang et al. reported the polysulfonamide-supported poly(ethylene glycol) divinyl ether-based SPE (PPDE-CPE), which was prepared via a cost-effective cationic polymerization induced by a small amount of LiBF₄. The PPDE-CPE possessed good flexibility and reliable mechanical stability for SMBs [77]. It was also found that the resultant PPDE-CPE exhibited an extended electrochemical stability window (4.7 V) and a relatively high ionic conductivity of 1.2 mS cm⁻¹ at room temperature. To further investigate the performance of the PPDE-CPE in sodium battery, NVP/Na half cells and MoS₂/Na half cells using PPDE-CPE were assembled and tested. The capacity retention of NVP/Na half-cell was 97.7% after 300 cycles at 3 C. The pouch-type cells consisting of MoS₂ anode, NVP cathode, and PPDE-CPE exhibited stable charge–discharge curves during 20 cycles, indicating promising applicability of the as-prepared PPDE-CPE for SMBs.

Besides the linear monomer, DOL, which is a typical cyclic monomer, can also be used to prepare SPE for SMBs through in-situ cationic polymerization. Niu et al. prepared a cross-linked polyether network (GPE-CPN) [78]. During the GPE-CPN preparation, in-situ copolymerization of trimethylolpropane triglycidyl ether (TMPTGE) and DOL were initiated by sodium hexafluorophosphate (NaPF₆) at room temperature. This copolymerization mechanism is vividly depicted in Figure 7a. The obtained GPE-CPN possessed good thermal stability (maintained its gelation state from 20 °C to 80 °C), enhanced ionic conductivity at ambient temperature (0.82 mS cm⁻¹), and a broad operating voltage window (4 V versus Na⁺/Na). The built NVP/Na cell employing GPE-CPN exhibited satisfactory capacity retention. Moreover, they found that the surface of the collected sodium is smooth after cycling during post-mortem morphology analysis. Additionally, the built NVP/pretreated hard carbon full cell using GPE-CPN also delivered a high-capacity retention. These results suggest stable interface between GPE-CPN and electrodes.

Although these results indicate that the GPE-CPN is very promising in building durable, safe, solid-state sodium batteries, its practical application in SMBs remains to be further studied (e.g., high-mass-loading sodium cathode coupled with high-mass-loading sodium anode). In the meantime, its electrochemical oxidation voltage is low to match high-voltage cathode materials (e.g., Na₃V₂(PO₄)₂O₂F, two stable high-voltage plateaus at 4.01 and 3.60 V), which is unfavorable to achieve high-energy-density SMBs. Therefore, some effective modification strategies are desirable to further widen its electrochemical stability window.

There can be more than one initiator during an in-situ polymerization process. Zhang et al. reported using the NaPF₆ and aluminum triflate (Al(OTf)₃) as co-initiators to initiate the in-situ polymerization of DOL for rechargeable SMBs [79]. No obvious polymerization can be detected when using either NaPF₆ or Al(OTf)₃ to induce the DOL polymerization. However, the polymerization reaction starts quickly when using these co-initiators simultaneously (0.15 M NaPF₆ and 2 mM Al(OTf)₃). It was found that both the Lewis acid Al(OTf)₃ and a trace amount of PF₅, resulting from the decomposition of NaPF₆, initiate the reaction. Both initiators were electrophilic, and the ring-opening polymerization of DOL did not occur unless both the initiators were attached to the oxygen atom in DOL. The obtained

SPE exhibited wide electrochemical stability, low volatility (80 wt% remaining after 23 h), improved ionic conductivity ($3.66 \times 10^{-4} \text{ S cm}^{-1}$ at room temperature), and sodium ion transference number (0.66).

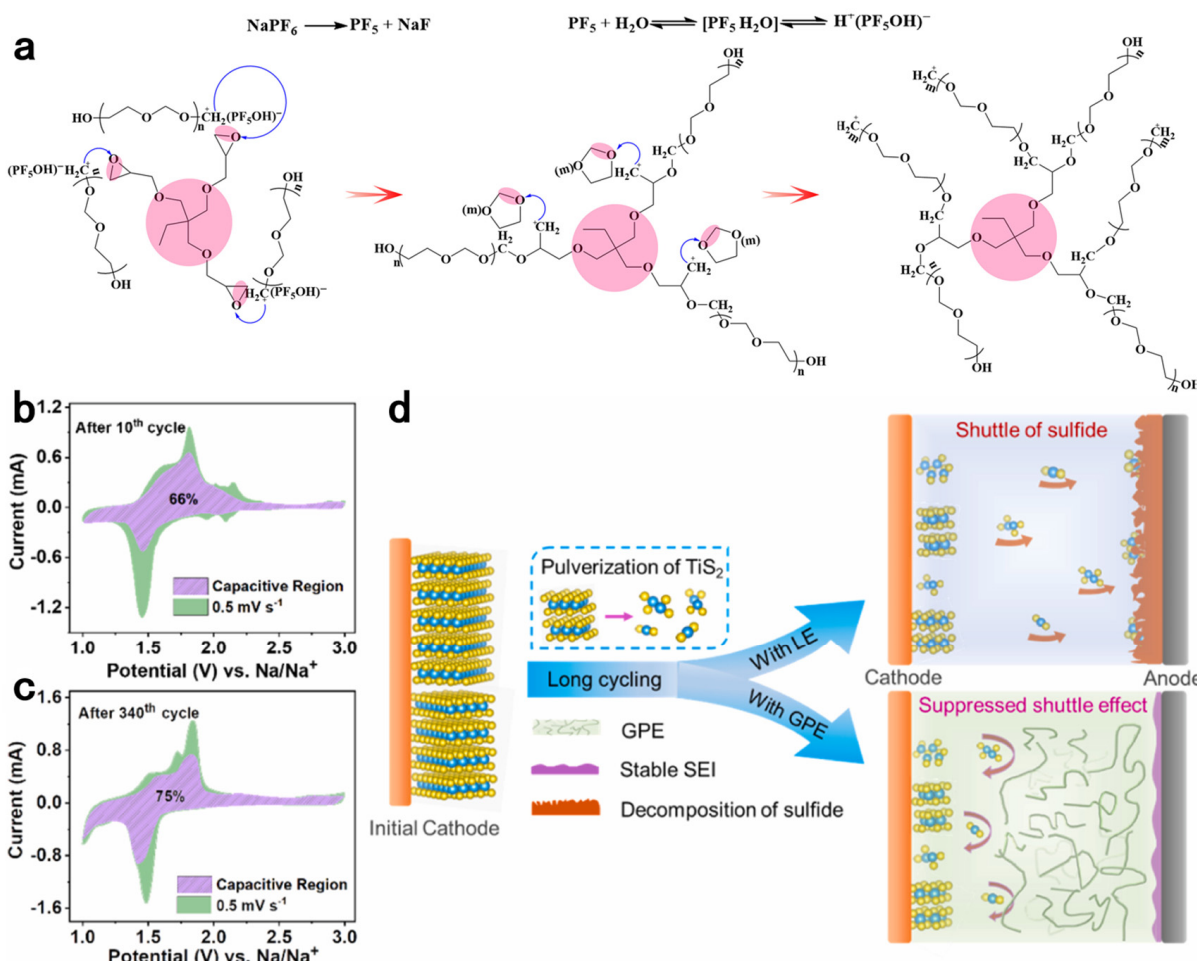


Figure 7. (a) Illustration of the polymerization of DOL and TMPTGE initiated by NaPF_6 . Reproduced with permission from [78]. The cyclic voltammetry (CV) curves at the scanning rate of 0.5 mV s^{-1} of the $\text{Na} \mid \text{TiS}_2$ cells after the 10th (b) and 340th (c) cycle. (d) Schematic explaining the $\text{TiS}_2 \mid \text{Na}$ cell using LE or SPE. Reproduced with permission from [79].

The electrochemical cycling test of the Na symmetrical batteries using the SPE proved long-term cyclability for 1300 h. Post-mortem scanning electron microscopy (SEM) images displayed that the plated Na was uniform and flat without obvious dendrites. Moreover, the cell displayed 371 mAh g^{-1} reversible capacity after 500 cycles (exceeding 6100 h). Furthermore, it was also found that this TiS_2/Na cell using the SPE displayed decreased interfacial resistance and overpotential after 1000 cycles. The remarkably improved battery performance was mainly ascribed to the good electrochemical compatibility and the inhibition of the shuttle effect (Figure 7b–d).

Overall, the in-situ cationic polymerization method is regarded as a facile and convenient solution to prepare SPEs for high-safety SMBs. Unfortunately, the polymerization degree via in-situ cationic polymerization is usually low (no more than 90%). The residual low-molecular-weight monomers may induce severe safety hazards. Therefore, the researchers are suggested to increase the polymerization degree and simultaneously develop flame-retardant SPEs via in-situ cationic polymerization.

5. SPEs Prepared through a Cross-Linking Reaction

Apart from the SMBs, Na-air batteries (one kind of SMBs, using Na anode and oxygen/air cathode) are also attracting great attention. However, the uncontrolled growth of Na dendrites, as well as the irreversible self-corrosion of Na, result in severe safety issues and rapid performance decay. As a result, controlling the Na electrodeposition and improving the structural stability of Na anode are essentially important for the further application of Na-air batteries.

To resolve the abovementioned issues, Liu et al. [80] demonstrated an NAB using an in-situ generated tetraethylene glycol dimethyl ether (G4)-based SPE initiated by Li ethylenediamine (LiEDA). As shown in Figure 8a,b, this SPE was obtained within the assembled NAB via cross-linking LiEDA at the anode surface in G4 in the liquid electrolyte. The reaction process is as follows: The Li reacts firstly with ethylenediamine (EDA) to produce a layer, and secondly the formed LiEDA is cross-linked with G4 to form a gel polymer electrolyte at the Na anode surface. After this reaction, residual trace amount of Li, which remains on the Na surface, is found to alloy with Na, and the formed Li–Na alloy is favorable for guiding uniform Na electrodeposition.

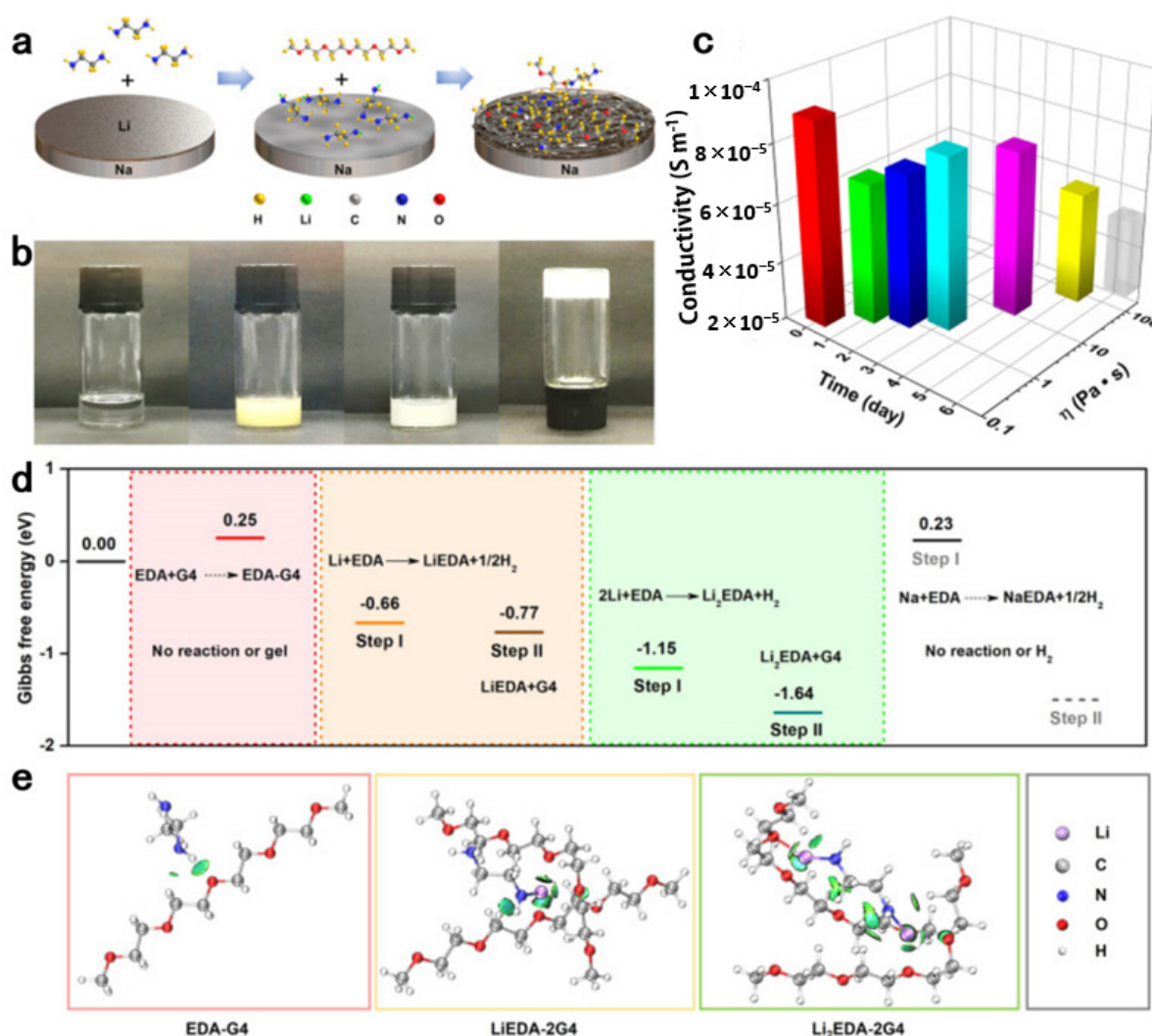


Figure 8. (a) Illustration explaining synthesizing the gel electrolyte. (b) Digital photos of the as-prepared gel electrolyte. (c) The measured ionic conductivity–viscosity–time evolution during manufacturing the gel electrolyte using 0.1 M NaCF_3SO_3 . (d) The calculated ΔG of potential reactions among Na, Li, EDA, G4, LiEDA, and Li_2EDA . (e) The selected LiEDA–2G4 and Li_2EDA –2G4 showing their structures. Reproduced with permission from [80].

As disclosed in Figure 8c, the formation of the gel occurred after 5 days, accompanied by decreased ionic conductivity. DFT calculation was used to disclose the possible gel formation mechanism (Figure 8d,e). As depicted in Figure 8d, the ΔG for generating LiEDA is negative, indicating a facile reaction between them. Moreover, Figure 8e shows that strong Li-O coordination bonds are detected in the LiEDA-2G4 and Li₂EDA-2G4, which are derived from cross-linking Li between LiEDA or Li₂EDA and the O from the G4.

The prepared gel polymer electrolyte can prevent O₂ and H₂O crossover, and hence, the Na anode corrosion can be inhibited. Moreover, the Na dendrites can be ameliorated by the well-known electrostatic shield effect of Li⁺. As a result, the NAB using this gel electrolyte delivered stable cycling performance that surpasses previous reports. Apart from that, the in-situ formed SPE avoids liquid leakage during battery bending. This property is conducive to the development of wearable NABs. Overall, the in-situ formed G4-based SPEs initiated by Li ethylenediamine LiEDA can tremendously enhance the NAB performance.

6. Conclusions and Perspectives

The desire for high-energy-density and high-safety SMBs drives the continuous search for new kinds of SPEs, which possess high ionic conductivity at ambient temperature and superior interfacial compatibility with anodes/cathodes. And the in-situ polymerization technique is regarded as the most convenient, effective, and favorable method to yield these SPEs.

Up to date, a variety of dedicatedly designed SPEs prepared via in-situ polymerization methods have been reported. Hence, this review summarizes the recent key progress of a series of in-situ polymerized SPE for SMBs, with a special focus on their design, synthesis, and applications. In particular, this review summarizes the following in-situ polymerization methods: photoinduced in-situ polymerization, thermally initiated in-situ free radical polymerization, in-situ cationic polymerization, and cross-linking reaction. From the author's view, it seems that the in-situ cationic polymerization method is the most promising in-situ polymerization method because it can occur under relatively mild conditions without involving harsh external conditions such as heating or light. In addition, this method uses lithium salt or lithium metal as an initiator without resorting to additional initiators, avoiding the adverse effects of foreign impurities on the battery operation.

Despite these developments in SPEs via in-situ polymerization for high-safety SMBs, several challenging issues still remain in the following aspects:

1. Sodium salt containing large anions is crucial to improve sodium-ion transference and ionic conductivity. However, almost all of the SPEs employ small anion during the in-situ polymerization in the previous works. Small anions will lead to lower sodium-ion transference numbers and increase the polarization of polymer cells. Hence, it is necessary to design and prepare SPEs using sodium salts containing large anions in future research.
2. At present, the reported in-situ polymerization employs the glass fiber separator or other separators, which separate the positive and negative electrodes before the polymerization reaction occurs. Nevertheless, the homogeneity and the consistency of the polymerized product in either the coin cells or pouch cells are not well studied. The inhomogeneous polymerization may cause unwanted results that decrease the battery performance, e.g., uneven electrode reactions would cause severe localized degradations of the electrode materials. Hence, the polymerization reactions occurring inside the cells are worth investigating in future work.
3. With the rapid deployment of rechargeable batteries in harsh operating conditions, such as deep-sea, deep-space, and deep-ground, it is important to design and develop fluorine-free, environmentally friendly polymer electrolytes to build next-generation fluorine-free SMBs to meet these requirements.
4. Although many in-situ polymerization methods have been demonstrated successful for building solid-state sodium metal batteries, from a practical point of view, it

is the sodium ion batteries that employ carbon anode will be widely used in grid energy storage or low-speed EVs. Hence, it is suggested that great efforts are devoted to developing in-situ polymerization methods for sodium-ion batteries built with carbon-based anodes.

5. The interfacial compatibility of the SPEs with both sodium anode and high-voltage cathode is crucially important to achieve high-energy-density and high-safety SIBs. Therefore, more ingenious and advanced characterization methods (e.g., synchrotron X-ray tomography, in-situ X-ray diffraction, operando nuclear magnetic resonance, in-situ Fourier-transform infrared, in-situ X-ray absorption near-edge structure) are necessary to further explore the interfacial compatibility and its dynamic evolution, which can provide mechanistic insights for developing advanced SPEs for SMBs.

Author Contributions: Conceptualization, G.C.; writing—original draft preparation, S.H., H.Z., S.T. and Y.Z.; writing—review and editing, D.W., Z.Y., B.Z., Y.H., J.Z. and G.C.; funding acquisition, J.Z. All authors have read and agreed to the published version of the manuscript.

Funding: This work was financially supported by the National Natural Science Foundation of China (Nos. 52073298, 52273221), the Youth Innovation Promotion Association of CAS (2020217) and Open Fund of Jiangsu Key Laboratory of Electrochemical Energy Storage Technologies No. EEST2022-1.

Data Availability Statement: Data sharing is not applicable to this article.

Conflicts of Interest: The authors declare no conflict of interest.

References

1. Tomich, A.W.; Park, J.; Son, S.-B.; Kamphaus, E.P.; Lyu, X.; Dogan, F.; Carta, V.; Gim, J.; Li, T.; Cheng, L.; et al. A carboranyl electrolyte enabling highly reversible sodium metal anodes via a “fluorine-free” SEI. *Angew. Chem. Int. Ed.* **2022**, *61*, e20220. [[CrossRef](#)] [[PubMed](#)]
2. Jin, Y.; Xu, Y.B.; Le, P.M.L.; Vo, T.D.; Zhou, Q.; Qi, X.G.; Engelhard, M.H.; Matthews, B.E.; Jia, H.; Nie, Z.M.; et al. Highly reversible sodium ion batteries enabled by stable electrolyte-electrode interphases. *ACS Energy Lett.* **2020**, *5*, 3212–3220. [[CrossRef](#)]
3. Ruiz-Martínez, D.; Gómez, R. Sulfur dioxide and sulfolane as additives in organic electrolytes to develop room-temperature sodium batteries. *Batteries* **2022**, *8*, 127. [[CrossRef](#)]
4. Singh, P.; Dixit, M. Opportunities and challenges in the development of layered positive electrode materials for high-energy sodium ion batteries: A computational perspective. *Langmuir* **2023**, *39*, 28–36. [[CrossRef](#)] [[PubMed](#)]
5. Song, K.M.; Liu, C.T.; Mi, L.W.; Chou, S.L.; Chen, W.H.; Shen, C.Y. Recent progress on the alloy-based anode for sodium-ion batteries and potassium-ion batteries. *Small* **2021**, *17*, 26. [[CrossRef](#)] [[PubMed](#)]
6. Park, S.; Park, S.; Mathew, V.; Sambandam, B.; Hwang, J.Y.; Kim, J. A new tellurium-based Ni_3TeO_6 -carbon nanotubes composite anode for Na-ion battery. *Int. J. Energy Res.* **2022**, *46*, 16041–16049. [[CrossRef](#)]
7. Fang, H.Y.; Suning Gao, S.N.; Ren, M.; Huang, Y.H.; Cheng, F.Y.; Chen, J.; Li, F.J. Dual-function presodiation with sodium diphenyl ketone towards ultra-stable hard carbon anodes for sodium-ion batteries. *Angew. Chem. Int. Ed.* **2023**, *62*, e202214717. [[CrossRef](#)]
8. Peng, J.; Zhang, W.; Liu, Q.N.; Wang, J.Z.; Chou, S.L.; Liu, H.K.; Dou, S.X. Prussian blue analogues for sodium-ion batteries: Past, present, and future. *Adv. Mater.* **2022**, *34*, 2108384. [[CrossRef](#)]
9. Zhu, Y.S.; Yao, Q.; Shao, R.W.; Wang, C.; Yan, W.S.; Ma, J.Z.; Liu, D.; Yang, J.; Qian, Y.T. Microsized gray tin as a high-rate and long-life anode material for advanced sodium-ion batteries. *Nano Lett.* **2022**, *22*, 7976–7983. [[CrossRef](#)]
10. Ali, Z.; Asif, M.; Huang, X.X.; Tang, T.Y.; Hou, Y.L. Hierarchically porous Fe_2CoSe_4 binary-metal selenide for extraordinary rate performance and durable anode of sodium-ion batteries. *Adv. Mater.* **2018**, *30*, 1802745. [[CrossRef](#)]
11. Hou, P.Y.; Sun, Y.Y.; Li, F.; Sun, Y.M.; Deng, X.L.; Zhang, H.Z.; Xu, X.J.; Zhang, L.Q. A high energy-density $\text{P}_2\text{Na}_{2/3}[\text{Ni}_{0.3}\text{Co}_{0.1}\text{Mn}_{0.6}]\text{O}_2$ cathode with mitigated $\text{P}_2\text{-O}_2$ transition for sodium-ion batteries. *Nanoscale* **2019**, *11*, 2787–2794. [[CrossRef](#)]
12. Zhang, W.C.; Lu, J.; Guo, Z.P. Challenges and future perspectives on sodium and potassium ion batteries for grid-scale energy storage. *Mater. Today* **2021**, *50*, 400–417. [[CrossRef](#)]
13. Li, X.; Sun, X.H.; Hu, X.D.; Fan, F.R.; Cai, S.; Zheng, C.M.; Stucky, G.D. Review on comprehending and enhancing the initial Coulombic efficiency of anode materials in lithium-ion/sodium-ion batteries. *Nano Energy* **2020**, *77*, 105143. [[CrossRef](#)]
14. Che, H.Y.; Chen, S.L.; Xie, Y.Y.; Wang, H.; Amine, K.; Liao, X.-Z.; Ma, Z.-F. Electrolyte design strategies and research progress for room-temperature sodium-ion batteries. *Energy Environ. Sci.* **2017**, *10*, 1075–1101. [[CrossRef](#)]
15. Wang, S.; Jiang, Y.J.; Hu, X.L. Ionogel-based membranes for safe lithium/sodium Batteries. *Adv. Mater.* **2022**, *34*, 2200945. [[CrossRef](#)]
16. Wang, Y.; Song, S.; Xu, C.; Hu, N.; Molenda, J.; Lu, L. Development of solid-state electrolytes for sodium-ion battery—A short review. *Nano Mater. Sci.* **2019**, *1*, 91–100. [[CrossRef](#)]

17. Monti, D.; Ponrouch, A.; Palacin, M.R.; Johansson, P. Towards safer sodium-ion batteries via organic solvent/ionic liquid based hybrid electrolytes. *J. Power Sources* **2016**, *324*, 712–721. [[CrossRef](#)]
18. Ma, Q.; Tietz, F. Solid-state electrolyte materials for sodium batteries: Towards practical applications. *ChemElectroChem* **2020**, *7*, 2693–2713. [[CrossRef](#)]
19. Gao, S.; Zhou, M.; Han, J.; Guo, C.; Tan, Y.; Jiang, K.; Wang, K. Progress on polymer electrolyte in sodium ion batteries. *Energy Storage Sci. Technol.* **2020**, *9*, 1300–1308.
20. Su, Y.; Rong, X.H.; Gao, A.; Liu, Y.; Li, J.W.; Mao, M.L.; Qi, X.G.; Chai, G.L.; Zhang, Q.H.; Suo, L.M.; et al. Rational design of a topological polymeric solid electrolyte for high-performance all-solid-state alkali metal batteries. *Nat. Commun.* **2022**, *13*, 4181. [[CrossRef](#)]
21. Lei, D.N.; He, Y.-B.; Huang, H.J.; Yuan, Y.F.; Zhong, G.M.; Zhao, Q.; Hao, X.G.; Zhang, D.F.; Lai, C.; Zhang, S.W.; et al. Cross-linked beta alumina nanowires with compact gel polymer electrolyte coating for ultra-stable sodium metal battery. *Nat. Commun.* **2019**, *10*, 4244. [[CrossRef](#)] [[PubMed](#)]
22. Yu, X.W.; Xue, L.G.; Goodenough, J.B.; Manthiram, A. Ambient-temperature all-solid-state sodium batteries with a laminated composite electrolyte. *Adv. Funct. Mater.* **2021**, *31*, 2002144. [[CrossRef](#)]
23. Yang, J.F.; Zhang, M.; Chen, Z.; Du, X.F.; Huang, S.Q.; Tang, B.; Dong, T.T.; Wu, H.; Yu, Z.; Zhang, J.J.; et al. Flame-retardant quasi-solid polymer electrolyte enabling sodium metal batteries with highly safe characteristic and superior cycling stability. *Nano Res.* **2019**, *12*, 2230–2237. [[CrossRef](#)]
24. Yin, H.; Han, C.J.; Liu, Q.R.; Wu, F.Y.; Zhang, F.; Tang, Y.B. Recent advances and perspectives on the polymer electrolytes for sodium/potassium-ion batteries. *Small* **2021**, *17*, 2006627. [[CrossRef](#)]
25. Natarajan, S.; Subramanyan, K.; Aravindan, V. Focus on spinel $\text{Li}_4\text{Ti}_5\text{O}_{12}$ as insertion type anode for high-performance Na-ion batteries. *Small* **2019**, *15*, 1904484. [[CrossRef](#)]
26. Liang, H.P.; Chen, Z.; Dong, X.; Zinkevich, T.; Indris, S.; Passerini, S.; Bresser, D. Photo-cross-linked single-ion conducting polymer electrolyte for lithium-metal batteries. *Macromol. Rapid Commun.* **2022**, *43*, 2100820. [[CrossRef](#)]
27. Dong, X.; Liu, X.; Li, H.H.; Passerini, S.; Bresser, D. Single-ion conducting polymer electrolyte for superior sodium metal batteries. *Angew. Chem. Int. Ed.* **2023**, *62*, e202308699. [[CrossRef](#)] [[PubMed](#)]
28. Zamory, J.; Bedu, M.; Fantini, S.; Passerini, S.; Paillard, E. Polymeric ionic liquid nanoparticles as binder for composite Li-ion electrodes. *J. Power Sources* **2013**, *240*, 745–752. [[CrossRef](#)]
29. Olmedo-Martínez, J.L.; Meabe, L.; Riva, R.; Guzmán-González, G.; Porcarelli, L.; Forsyth, M.; Mugica, A.; Calafel, I.; Müller, A.J.; Lecomte, P.; et al. Flame retardant polyphosphoester copolymers as solid polymer electrolyte for lithium batteries. *Polym. Chem.* **2021**, *12*, 3441. [[CrossRef](#)]
30. Nair, J.R.; Bella, F.; Angulkshmi, N.; Stephan, A.M.; Gerbaldi, C. Nanocellulose-laden composite polymer electrolytes for high performing lithium–sulphur batteries. *Energy Storage Mater.* **2016**, *3*, 69–76. [[CrossRef](#)]
31. Nair, J.R.; Destro, M.; Bella, F.; Appetecchi, G.B.; Gerbaldi, C. Thermally cured semi-interpenetrating electrolyte networks (s-IPN) for safe and aging-resistant secondary lithium polymer batteries. *J. Power Sources* **2016**, *306*, 258–267. [[CrossRef](#)]
32. Li, J.Y.; Zhu, H.J.; Wang, X.E.; Armand, M.; MacFarlane, D.R.; Forsyth, M. Synthesis of sodium poly [4-styrenesulfonyl(trifluoromethylsulfonyl)imide]-co-ethylacrylate] solid polymer electrolytes. *Electrochim. Acta* **2015**, *175*, 232–239. [[CrossRef](#)]
33. Mogensen, R.; Brandell, D.; Younesi, R. Solubility of the solid electrolyte interphase (SEI) in sodium ion batteries. *ACS Energy Lett.* **2016**, *1*, 1173–1178. [[CrossRef](#)]
34. Grundish, N.S.; Goodenough, J.B.; Khani, H. Designing composite polymer electrolytes for all-solid state lithium batteries. *Electrochemistry* **2021**, *30*, 100828. [[CrossRef](#)]
35. Chen, L.; Li, Y.T.; Li, S.P.; Fan, L.Z.; Nan, C.W.; Goodenough, J.B. PEO/garnet composite electrolytes for solid-state lithium batteries: From “ceramic-in-polymer” to “polymer-in-ceramic”. *Nano Energy* **2018**, *46*, 176–184. [[CrossRef](#)]
36. Fang, R.Y.; Li, Y.T.; Wu, N.; Xu, B.Y.; Liu, Y.J.; Manthiram, A.; Goodenough, J.B. Ultra-thin single-particle-layer sodium beta-alumina based composite polymer electrolyte membrane for sodium-metal batteries. *Adv. Funct. Mater.* **2023**, *33*, 2211229. [[CrossRef](#)]
37. Guo, J.Z.; Yang, A.B.; Gu, Z.Y.; Wu, X.L.; Pang, W.L.; Ning, Q.L.; Li, W.H.; Zhang, J.P.; Su, Z.M. Quasi-solid-state sodium-ion full battery with high-power/energy densities. *ACS Appl. Mater. Interfaces* **2018**, *10*, 17903–17910. [[CrossRef](#)]
38. Huang, Y.; Fang, C.; Zeng, R.; Liu, Y.J.; Zhang, W.; Wang, Y.J.; Liu, Q.J.; Huang, Y.H. In situ-formed hierarchical metal-organic flexible cathode for high-energy sodium-ion batteries. *ChemSusChem* **2017**, *10*, 4704–4708. [[CrossRef](#)]
39. Chae, W.; Kim, B.; Ryoo, W.S.; Earmme, T. A brief review of gel polymer electrolytes using in situ polymerization for lithium-ion polymer batteries. *Polymers* **2023**, *15*, 803. [[CrossRef](#)]
40. Zhao, Q.; Liu, X.T.; Stalin, S.; Khan, K.; Archer, L.A. Solid-state polymer electrolytes with in-built fast interfacial transport for secondary lithium batteries. *Nat. Energy* **2019**, *4*, 365–373. [[CrossRef](#)]
41. Liu, T.T.; Zhang, J.J.; Wu, H.; Zhang, J.N.; Ding, G.; Dong, S.M.; Cui, G.L. In situ polymerization for integration and interfacial protection towards solid state lithium batteries. *J. Electrochem. Soc.* **2020**, *167*, 070527. [[CrossRef](#)]
42. Zhang, Y.F.; Chen, Y.Z.; Liu, Y.; Qin, B.S.; Yang, Z.H.; Sun, Y.B.; Zeng, D.L.; Varzib, A.; Passerini, S.; Liu, Z.H.; et al. Highly porous single-ion conductive composite polymer electrolyte for high performance Li-ion batteries. *J. Power Sources* **2018**, *397*, 79–86. [[CrossRef](#)]

43. Nair, J.R.; Colò, F.; Kazzazi, A.; Moreno, M.; Bresser, D.; Lin, R.L.; Bella, F.; Meligrana, G.; Fantini, S.; Simonetti, E.; et al. Room temperature ionic liquid (RTIL)-based electrolyte cocktails for safe, high working potential Li-based polymer batteries. *J. Power Sources* **2019**, *412*, 398–407. [[CrossRef](#)]
44. Nair, J.R.; Cíntora-Juárez, D.; Pérez-Vicenteb, C.; Tiradob, J.L.; Ahmadc, S.; Gerbaldia, C. Truly quasi-solid-state lithium cells utilizing carbonate free polymer electrolytes on engineered LiFePO₄. *Electrochim. Acta* **2016**, *199*, 172–179. [[CrossRef](#)]
45. Noor, S.A.M.; Yoon, H.; Forsyth, M.; MacFarlane, D.R. Gelled ionic liquid sodium ion conductors for sodium batteries. *Electrochim. Acta* **2015**, *169*, 376–381. [[CrossRef](#)]
46. Sun, B.; Liao, I.-Y.; Tan, S.; Bowden, T.; Brandell, D. Solid polymer electrolyte coating from a bifunctional monomer for three-dimensional microbattery applications. *J. Power Sources* **2013**, *238*, 435–441. [[CrossRef](#)]
47. Fang, R.Y.; Xu, B.Y.; Grundish, N.S.; Xia, Y.; Li, Y.T.; Lu, C.W.; Yijie Liu, Y.J.; Wu, N.; Goodenough, J.B. Li₂S₆-integrated PEO-based polymer electrolytes for all-solid-state lithium-metal batteries. *Angew. Chem. Int. Ed.* **2021**, *60*, 17701–17706. [[CrossRef](#)]
48. Khani, H.; Kalami, S.; Goodenough, J.B. Micropores-in-macroporous gel polymer electrolytes for alkali metal batteries. *Sustain. Energ. Fuels* **2020**, *4*, 177. [[CrossRef](#)]
49. Meisner, Q.J.; Jiang, S.S.; Cao, P.F.; Glossmann, T.; Hintennach, A.; Zhang, Z.C. An in situ generated polymer electrolyte via anionic ring-opening polymerization for lithium-sulfur batteries. *J. Mater. Chem. A* **2021**, *9*, 25927–25933. [[CrossRef](#)]
50. Vijayakumar, V.; Anothumakkool, B.; Kurungot, S.; Winter, M.; Nair, J.R. In situ polymerization process: An essential design tool for lithium polymer batteries. *Energy Environ. Sci.* **2021**, *14*, 2708–2788. [[CrossRef](#)]
51. Ma, J.; Feng, X.Y.; Wu, Y.Y.; Wang, Y.D.; Liu, P.C.; Shang, K.; Jiang, H.; Hou, X.L.; Mitlin, D.; Xiang, H.F. Stable sodium anodes for sodium metal batteries (SMBs) enabled by in-situ formed quasi solid-state polymer electrolyte. *J. Energy Chem.* **2023**, *77*, 290–299. [[CrossRef](#)]
52. Yang, J.F.; Zhang, H.R.; Zhou, Q.; Qu, H.T.; Dong, T.T.; Zhang, M.; Tang, B.; Zhang, J.J.; Cui, G.L. Safety-enhanced polymer electrolytes for sodium batteries: Recent progress and perspectives. *ACS Appl. Mater. Interfaces* **2019**, *11*, 17109–17127. [[CrossRef](#)]
53. Zheng, J.Y.; Li, W.J.; Liu, X.X.; Zhang, J.W.; Feng, X.M.; Chen, W.H. Progress in gel polymer electrolytes for sodium-ion batteries. *Energy Environ. Mater.* **2022**, *6*, e12422. [[CrossRef](#)]
54. Gebert, F.; Knott, J.; Gorkin III, R.; Chou, S.-L.; Dou, S.-X. Polymer electrolytes for sodium-ion batteries. *Energy Storage Mater.* **2021**, *36*, 10–30. [[CrossRef](#)]
55. Qiao, L.X.; Judez, X.; Rojo, T.; Armand, M.; Zhang, H. Polymer electrolytes for sodium batteries. *J. Electrochem. Soc.* **2020**, *167*, 070534. [[CrossRef](#)]
56. Bella, F.; Colý, F.; Nair, J.R.; Gerbaldi, C. Photopolymer electrolytes for sustainable, upscalable, safe, and ambient-temperature sodium-ion secondary batteries. *ChemSusChem* **2015**, *8*, 3668–3676. [[CrossRef](#)] [[PubMed](#)]
57. Yao, Y.; Wei, Z.Y.; Wang, H.Y.; Huang, H.J.; Jiang, Y.; Wu, X.J.; Yao, X.Y.; Wu, Z.-S.; Yu, Y. Toward high energy density all solid-state sodium batteries with excellent flexibility. *Adv. Energy Mater.* **2020**, *10*, 1903698. [[CrossRef](#)]
58. Wen, P.C.; Lu, P.F.; Shi, X.Y.; Yao, Y.; Shi, H.D.; Liu, H.Q.; Yu, Y.; Wu, Z.-S. Photopolymerized gel electrolyte with unprecedented room-temperature ionic conductivity for high-energy density solid-state sodium metal batteries. *Adv. Energy Mater.* **2021**, *11*, 2002930. [[CrossRef](#)]
59. Zhou, D.; Chen, Y.; Li, B.H.; Fan, H.B.; Cheng, F.L.; Shanmukaraj, D.; Rojo, T.; Armand, M.; Wang, G.X. A stable quasi-solid-state sodium-sulfur battery. *Angew. Chem. Int. Ed.* **2018**, *57*, 10168–10172. [[CrossRef](#)] [[PubMed](#)]
60. Qin, H.; Panzer, M.J. Zwitterionic copolymer-supported ionogel electrolytes featuring a sodium salt/ionic liquid solution. *Chem. Mater.* **2020**, *32*, 7951–7957. [[CrossRef](#)]
61. Kim, J.; Choi, Y.G.; Ahn, Y.; Kim, D.; Park, J.H. Optimized ion-conductive pathway in UV-cured solid polymer electrolytes for all-solid lithium/sodium ion batteries. *J. Membr. Sci.* **2021**, *619*, 118711. [[CrossRef](#)]
62. Chen, S.L.; Che, H.Y.; Feng, F.; Liao, J.P.; Wang, H.; Yin, Y.M. Poly(vinylene carbonate)-based composite polymer electrolyte with enhanced interfacial stability to realize high-performance room temperature solid-state sodium batteries. *ACS Appl. Mater. Interfaces* **2019**, *11*, 43056–43065. [[CrossRef](#)]
63. Gao, H.C.; Zhou, W.D.; Park, K.; Goodenough, J.B. A sodium-ion battery with a low-cost cross-linked gel-polymer electrolyte. *Adv. Energy Mater.* **2016**, *6*, 1600467. [[CrossRef](#)]
64. Zhou, Y.-N.; Xiao, Z.C.; Han, D.Z.; Yang, L.P.; Zhang, J.Y.; Tang, W.; Shu, C.Y.; Peng, C.X.; Zhou, D.P. Approaching practically accessible and environmentally adaptive sodium metal batteries with high loading cathodes through in situ interlock interface. *Adv. Funct. Mater.* **2022**, *32*, 2111314. [[CrossRef](#)]
65. Zhang, W.C.; Zhang, J.; Liu, X.C.; Li, H.; Guo, Y.; Geng, C.N.; Tao, Y.; Yang, Q.-H. In-situ polymerized gel polymer electrolytes with high room-temperature ionic conductivity and regulated Na⁺ solvation structure for sodium metal batteries. *Adv. Funct. Mater.* **2022**, *32*, 2201205. [[CrossRef](#)]
66. Zhou, D.; Liu, R.L.; Zhang, J.; Qi, X.G.; He, Y.-B.; Li, B.H.; Yang, Q.H.; Hu, Y.-S.; Kang, F.Y. In situ synthesis of hierarchical poly(ionic liquid)-based solid electrolytes for high-safety lithium-ion and sodium-ion batteries. *Nano Energy* **2017**, *33*, 45–54. [[CrossRef](#)]
67. Chen, G.H.; Zhang, K.; Liu, Y.R.; Ye, L.; Gao, Y.S.; Lin, W.R.; Xu, H.J.; Wang, X.R.; Bai, Y.; Wu, C. Flame-retardant gel polymer electrolyte and interface for quasi-solid-state sodium ion batteries. *Chem. Eng. J.* **2020**, *401*, 126065. [[CrossRef](#)]

68. Park, T.-H.; Park, M.-S.; Ban, A.-H.; Lee, Y.-S.; Kim, D.-W. Nonflammable gel polymer electrolyte with ion-conductive polyester networks for sodium metal cells with excellent cycling stability and enhanced safety. *ACS Appl. Energy Mater.* **2021**, *4*, 10153–10162. [[CrossRef](#)]
69. Zheng, J.Y.; Zhao, Y.H.; Feng, X.M.; Chen, W.H.; Zhao, Y.F. Novel safer phosphonate-based gel polymer electrolytes for sodium-ion batteries with excellent cycling performance. *J. Mater. Chem. A* **2018**, *6*, 6559–6564. [[CrossRef](#)]
70. Zheng, J.Y.; Liu, X.L.; Duan, Y.L.; Chen, L.J.; Zhang, X.C.; Feng, X.M.; Chen, W.H.; Hao, Y.F. Stable cross-linked gel terpolymer electrolyte containing methyl phosphonate for sodium ion batteries. *J. Membrane Sci.* **2019**, *58*, 163–170. [[CrossRef](#)]
71. Zheng, J.Y.; Yang, Y.W.; Li, W.J.; Feng, X.M.; Chen, W.H.; Zhao, Y.F. Novel flame retardant rigid spirocyclic biphenylphosphate based copolymer gel electrolytes for sodium ion batteries with excellent high-temperature performance. *J. Mater. Chem. A* **2020**, *8*, 22962–22968. [[CrossRef](#)]
72. Zheng, J.Y.; Sun, Y.K.; Li, W.J.; Feng, X.M.; Chen, W.H.; Zhao, Y.F. Effects of comonomers on the performance of stable phosphonate-based gel terpolymer electrolytes for sodium-ion batteries with ultralong cycling stability. *ACS Appl. Mater. Interfaces* **2021**, *13*, 25024–25035. [[CrossRef](#)]
73. Yi, Q.; Zhang, W.; Li, S.; Li, X.; Sun, C. Durable sodium battery with a flexible $\text{Na}_3\text{Zr}_2\text{Si}_2\text{PO}_{12}$ -PVDF-HFP composite electrolyte and sodium/carbon cloth anode. *ACS Appl Mater Interfaces* **2018**, *10*, 35039–35046. [[CrossRef](#)]
74. Xu, X.; Lin, K.; Zhou, D.; Liu, Q.; Qin, X.; Wang, S.; He, S.; Kang, F.; Li, B.; Wang, G. Quasi-solid-state dual-ion sodium metal batteries for low-cost energy storage. *Chem* **2020**, *6*, 902–918. [[CrossRef](#)]
75. Li, W.; Yao, Z.; Zhang, S.; Wang, X.; Xia, X.; Gu, C.; Tu, J. High-performance $\text{Na}_3\text{V}_2(\text{PO}_4)_2\text{F}_{2.5}\text{O}_{0.5}$ cathode: Hybrid reaction mechanism study via ex-situ XRD and sodium storage properties in solid-state batteries. *Chem. Eng. J.* **2021**, *423*, 130310. [[CrossRef](#)]
76. Luo, C.; Li, Q.; Shen, D.; Zheng, R.; Huang, D.; Chen, Y. Enhanced interfacial kinetics and fast Na^+ conduction of hybrid solid polymer electrolytes for all-solid-state batteries. *Energy Storage Mater.* **2021**, *43*, 463–470. [[CrossRef](#)]
77. Zhang, J.J.; Wen, H.J.; Yue, L.P.; Chai, J.C.; Ma, J.; Hu, P.; Ding, G.L.; Wang, Q.F.; Liu, Z.H.; Cui, G.L.; et al. In situ formation of polysulfonamide supported poly(ethylene glycol) divinyl ether based polymer electrolyte toward monolithic sodium ion batteries. *Small* **2017**, *13*, 1601530. [[CrossRef](#)]
78. Niu, Y.B.; Yin, Y.X.; Wang, W.P.; Wang, P.F.; Ling, W.; Xiao, Y.; Guo, Y.G. In situ copolymerized gel polymer electrolyte with cross-linked network for sodium-ion batteries. *CCS Chem.* **2019**, *1*, 589–597. [[CrossRef](#)]
79. Zhang, X.Q.; Tang, S.; Li, X.; Guo, W.; Fu, Y.Z. Ultrastable Na-TiS₂ battery enabled by in situ construction of gel polymer electrolyte. *J. Power Sources* **2021**, *516*, 230653. [[CrossRef](#)]
80. Liu, X.Z.; Lei, X.F.; Wang, Y.-G.; Ding, Y. Prevention of Na corrosion and dendrite growth for long-life flexible Na-Air Batteries. *ACS Central Sci.* **2021**, *7*, 335–344. [[CrossRef](#)]

Disclaimer/Publisher's Note: The statements, opinions and data contained in all publications are solely those of the individual author(s) and contributor(s) and not of MDPI and/or the editor(s). MDPI and/or the editor(s) disclaim responsibility for any injury to people or property resulting from any ideas, methods, instructions or products referred to in the content.